Laboratory Observation of Electron Phase-Space Holes during Magnetic Reconnection

W. Fox, M. Porkolab, J. Egedal, N. Katz, and A. Le
Department of Physics, and Plasma Science and Fusion Center, Massachusetts Institute of Technology (MIT), Cambridge, Massachusetts 02139, USA
(Received 30 July 2008; published 18 December 2008)

We report the observation of large-amplitude, nonlinear electrostatic structures, identified as electron phase-space holes, during magnetic reconnection experiments on the Versatile Toroidal Facility at MIT. The holes are positive electric potential spikes, observed on high-bandwidth ($\sim$2 GHz) Langmuir probes. Investigations with multiple probes establish that the holes travel at or above the electron thermal speed and have a three-dimensional, approximately spherical shape, with a scale size $\sim$2 mm. This corresponds to a few electron gyroradii, or many tens of Debye lengths, which is large compared to holes considered in simulations and observed by satellites, whose length scale is typically only a few Debye lengths. Finally, a statistical study over many discharges confirms that the holes appear in conjunction with the large inductive electric fields and the creation of energetic electrons associated with the magnetic energy release.

DOI: 10.1103/PhysRevLett.101.255003 PACS numbers: 52.35.Sb, 52.35.Vd

Electron phase-space holes [1,2], also called Bernstein-Greene-Kruskal (BGK) solitary structures, are the self-consistent plasma structures that form when a finite number of particles become trapped in large-amplitude plasma waves. They play a role in a number of plasma processes, most importantly the nonlinear saturation of velocity-space (two-stream) instabilities. The ''BGK state''—where initial linear modes have evolved into an ensemble of these BGK structures—also appears in the saturation of Landau damping [3]. Electron holes have received substantial attention lately due to a recent generation of spacecraft which has found them to be nearly ubiquitous in the space environment [4,5]. However, their practical consequences extend across the spectrum of plasma physics to also include, for instance, laser-plasma interactions relevant to inertial confinement fusion [6].

Holes are inherently nonlinear plasma structures, consisting of a positive-potential spike which has trapped a population of electrons. The kinetic, Vlasov description of hole equilibria was established by Bernstein, Greene, and Kruskal [1]. Later, Berk and collaborators showed that these structures appeared in simulations of the two-stream instability when the instability saturated by particle trapping [7]. Recent progress, driven by space observations, has extended the original 1D theory to higher dimensions, in both dynamical simulations (e.g., [8]) and with analytic equilibria (e.g., [9]), and has established agreement between theory and observations [10]. The dynamics of holes have also been studied in dedicated laboratory experiments [11].

Because of their presence in the turbulent, saturated state of instabilities, electron holes may also play an important role in magnetic reconnection processes. Primarily, current-driven turbulence is studied for its ability to provide ''anomalous resistivity'' to the plasma, speeding the reconnection rate [12]. Drake *et al.* [13] have found electron holes resulting from electron-ion (Buneman) instability in reconnection simulations and found that they were indeed a source of anomalous resistivity. In space observations, holes associated with reconnection have now been observed both at the bow shock and in the magnetotail [14,15].

Here we report the laboratory observation of electron holes within the electrostatic turbulence created during spontaneous reconnection events on the Versatile Toroidal Facility (VTF) [16]. The holes are observed on high-bandwidth, single-ended Langmuir probes as positive spikes of large amplitude. In these experiments, a plasma current sheet is induced by changing the currents in toroidal coils fixed inside the vacuum chamber. The current sheet accumulates magnetic energy until a reconnection event releases the energy over a short period of time. The electron holes are observed in conjunction with the large inductive electric fields and energetic particle creation associated with this magnetic energy release.

In contrast to previous laboratory studies [11], where the perpendicular size of the holes was set by the plasma boundary, here the holes are small compared to the size of the experiment, so plasma processes will control the holes' three-dimensional shape. We find that the holes formed are, in fact, 3D structures and are approximately spherical with a scale size of a few electron gyroradii. Our observations also indicate that the holes in VTF most likely arise from *electron-electron* velocity-space instability. The holes are but one type of fluctuation that we have observed during reconnection on this experiment; studies of other types of fluctuations will appear in forthcoming papers.

Figure 1(a) shows the poloidal cross section of the toroidal VTF device, including a few vacuum flux surfaces (i.e., poloidal projection of the magnetic field lines). As in previous research [16], a current sheet and subsequent reconnection are induced in the plasma by quickly chang-

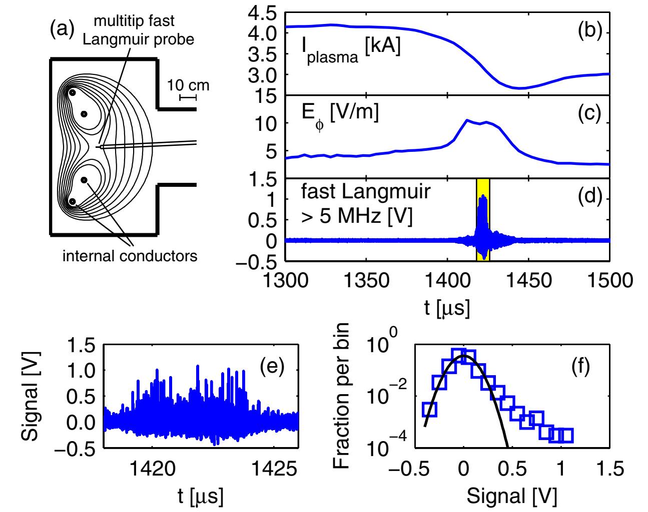

FIG. 1 (color online). (a) A schematic of the experiment at one poloidal cross section. (b) Total plasma current, (c) toroidal-averaged toroidal electric field, and (d) fluctuation trace for the time period 1300–1500 μs. (e) Zoom-in on the fluctuation trace from 1418 to 1426 μs. (f) Log-histogram of voltages measured by fluctuation probe over this time period. The black curve indicates a best Gaussian fit to the central portion of the data; it is parabolic on the log scale.

ing the currents in the internal conductors. We attain (argon) plasma densities of (1–2) $\times 10^{18}$ m^{-3} and electron temperatures of approximately 15 eV. The toroidal, "guide" magnetic field B_ϕ—50–70 mT at the major radius (0.92 m) of the reconnection x line—dominates $B_{\rm up}$, the typically 5 mT, poloidal, reconnecting component of the field. To supplement the 2D magnetic [17] and Langmuir probe diagnostic arrays in VTF, we have added high-bandwidth, "fast" Langmuir probes to observe electrostatic fluctuations in the plasma. They are impedance-matched at 50 Ω and digitized by an oscilloscope, which can simultaneously digitize up to 4 channels to study the propagation of observed modes.

Figures 1(b)–1(d) show (b) typical time traces of total plasma current, (c) toroidal-averaged, toroidal, "reconnection" electric field E_ϕ, and (d) fluctuations from one of the fast Langmuir probes, positioned within a few centimeters of the reconnection x line. In this particular discharge, the reconnection event occurred from $t = 1410$ to 1440 μs, during which time the plasma current fell by nearly half. The reconnection electric field reached 10 V/m, and the reconnection inflow rate $v_{\rm in} = E_\phi / B_{\rm up}$ reached approximately $0.1 V_{A,{\rm up}}$, where $V_{A,{\rm up}} = B_{\rm up}/\sqrt{\mu_0 n m_i}$ [16].

Strong electrostatic fluctuations are generally observed to arise during the reconnection events. Figure 1(e) shows the fluctuations over a shorter time window, and Fig. 1(f) shows a histogram of the measured voltages over this time. Over the shorter time period, asymmetric, positive-potential "spikes" can clearly be seen. For the histogram, if the fluctuations were simply broadband white noise, we would find that the distribution of measured voltages should be simply Gaussian. Instead, the spikes form an extended, non-Gaussian tail on the distribution of fluctuations; it is these spikes which are the electron holes.

We conducted further experiments to study the spikes in detail using a set of fast Langmuir probes with small, 60-μm-diameter tips, arrayed at various separations from one another ranging from 0.8 to 8 mm. The probe can be rotated so that the tips can be separated either parallel or perpendicular to the field.

Figure 2(a) shows a 200 ns trace on a pair of fast Langmuir probes, separated by 4.6 mm in the toroidal direction, essentially parallel to the magnetic field. Figure 2(b) zooms in on a smaller 10 ns window which contains two spike pairs. The data points, sampled at 5 GS/s, appear as open symbols. The spikes are well-correlated between the two probe tips, with a time delay of about 1.2 ns. Other tests with the probes separated perpendicular to the magnetic field show zero time delay, indicating that the spikes travel *along* the magnetic field. Finally, in Fig. 2(b), the green trace with square symbols is from the "upstream" probe—upstream in terms of the electron flow inferred from the total plasma current—indicating that the spikes travel along the magnetic field *with* the electron flow.

Next, we measure the spikes' propagation speed from time delays between probe tips. The histogram in Fig. 2(c) shows the distribution of measured delays for all spikes observed during this discharge; the typical delay between the two probes is about 1.2 ns. Based on the 4.6 mm probe separation, we find that the spikes travel nearly 4×10^6 m/s. In plasma units this is approximately $1.5 v_{\rm te}$, where $v_{\rm te} = \sqrt{2kT_e/m_e}$ has been evaluated using the typical 15 eV. This speed is substantially larger than the average electron parallel drift (evaluated from the total plasma current) $v_{\rm de} \simeq 0.1 v_{\rm te}$ but is in the range to interact

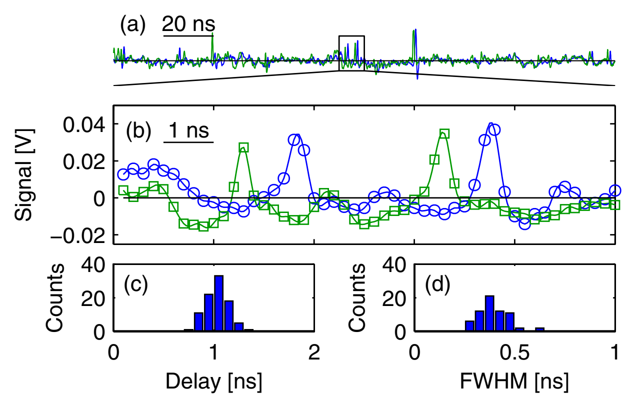

FIG. 2 (color online). (a) A pair of fluctuation traces over a 200 ns window and (b) a 10 ns window. The probes are separated by 4.6 mm parallel to the magnetic field. (c) Histogram of probe-probe delays for the spikes. (d) Histogram of measured spike temporal widths (FWHM).

with high energy electrons produced by magnetic reconnection. This will be elaborated below.

The parallel size of the spikes can now be measured based on the inferred speed and the temporal width of the trace. The spikes from Fig. 2(b) have full-width-half-maximum (FWHM) temporal widths of about 500 ps. Figure 2(d) shows the statistics of the parallel widths measured for all spikes found during this discharge; the typical temporal width is about 400 ps. Combining this typical width and the spike velocity, we infer a typical parallel diameter of 1.5 mm. In plasma units, this is 8 gyroradii ($\rho_e = v_{\rm te}/\omega_{\rm ce} \approx 200\ \mu$m). Alternatively, this is about 60 Debye lengths ($\lambda_D = \sqrt{\epsilon_0 kT_e/ne^2} \approx 25\ \mu$m). Note that this is also much wider than the probe diameter.

We now turn to experiments with the probe tips separated perpendicular to the magnetic field, which we use to measure the perpendicular size of the spikes. Figure 3 shows histograms comparing signals observed by pairs of probes at zero time delay. Integrating in the vertical or horizontal directions on any plot gives the single-probe histograms, which are shown in log scale exactly as in Fig. 1(e). As noted before, the tail of outliers on the scatter plots and log-histograms (where the log-histograms deviate from being parabolic) are the spikes. As is readily visible from the plots, the outliers or spikes at $\Delta =$ 0.8 mm (top left) are highly correlated, implying the spikes must be typically larger than 0.8 mm. The same exercise can be repeated for increasing probe separations. Of note, at $\Delta = 4.6$ mm (bottom right), there is essentially no correlation between the outliers. These measurements thus bracket the typical perpendicular size of the spikes, which we take as 2 mm. As this is similar to the parallel size, the spikes are approximately spherical.

Finally, we estimate that potentials associated with the spikes are of order kT_e/e. We model the plasma-probe

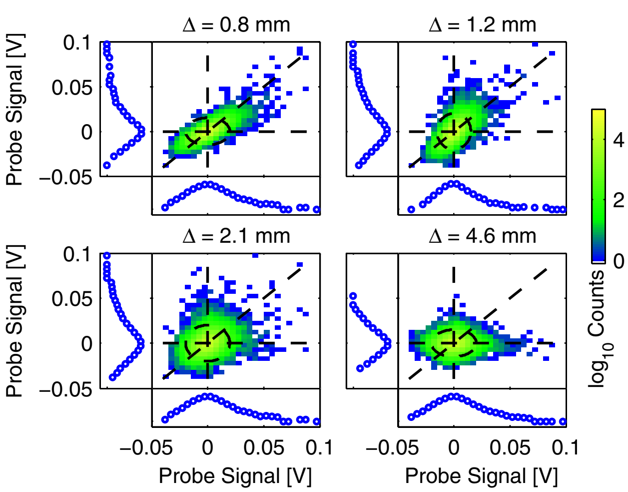

FIG. 3 (color online). Probe-probe correlation histograms and corresponding single-probe log-histograms at zero time delay. The probe separations range from 0.8 to 4.6 mm perpendicular to the magnetic field.

coupling as a parallel sheath resistance and capacitance [18]; these form a voltage divider with the 50-Ω termination. We typically use an rf blocking capacitor in series with the 50-Ω load to allow the probe tips to "float" on long time scales (10 μs). The sheath resistance is therefore related to the probe I-V curve near the floating potential and is typically 4 kΩ. The parallel capacitance is estimated to make about equal contribution on the spike time scales. Using this model, we estimate $\phi \sim 20$ V $\sim kT_e/e$ based on spike amplitudes in the range of 500 mV (see Fig. 1).

Our observations favor electron holes over other nonlinear plasma structures, such as envelope solitons [19] or Korteweg–de Vries-type fluid solitons. Primarily, this is based on their polarity ($e\phi > 0$, consistent with holes and inconsistent with fluid solitons [20]), supersonic speed, and lack of internal "pump-wave" oscillations (as would be expected in an envelope soliton). That said, while the perpendicular size is in agreement with other electron hole observations, the parallel diameter is large and the velocity somewhat higher, points which we now address.

First, the typical perpendicular size of the observed electron holes (a few ρ_e) is in agreement with available space observations and theoretical considerations. Franz *et al.* [21] have presented a statistical study of the inferred parallel and perpendicular sizes of electron holes measured by the Polar spacecraft. The critical parameter here is $\omega_{\rm pe}/\omega_{\rm ce}$ or, equivalently, ρ_e/λ_D. They found that the perpendicular size transitioned from being a few λ_D when $\omega_{\rm pe}/\omega_{\rm ce} \leq 1$ to being a few ρ_e when $\omega_{\rm pe}/\omega_{\rm ce} \geq 1$. This concurs with our measurements of ρ_e-scale holes, as VTF is in the latter regime $\omega_{\rm pe}/\omega_{\rm ce} \sim 10$. Theory also predicts that ρ_e sets a minimum perpendicular size: An electron hole equilibrium requires that a positive potential cause a depletion of electrons, which results only when the electrons obey a magnetized, 1D response along the field lines. (See Ref. [9] for essentially a proof of this.) To keep the electrons magnetized, the hole's perpendicular size must be at least a few gyroradii.

On the other hand, the typical *parallel* size of holes observed by spacecraft [4,5,21] is nearly always a few Debye lengths. This is much narrower than the holes we have observed, which are roughly $60\lambda_D$ wide. However, holes this wide are not theoretically forbidden: In fact, calculations show that holes become wide ($\gg \lambda_D$) when they move at high speeds ($v_{\rm hole} \approx v_{\rm te}$) [10]. This is qualitatively consistent with the measurements here in that we observe holes that are both wide and fast. More detailed comparisons will await improved measurements of the electron distribution function.

To verify a connection among electron holes, the reconnection electric field, and the production of high energy electrons, we have constructed a gridded electron energy analyzer with 7 independent grid/collector pairs within a small region of about 1.5 cm. This probe observes fluxes of high energy electrons with time response on the reconnec-

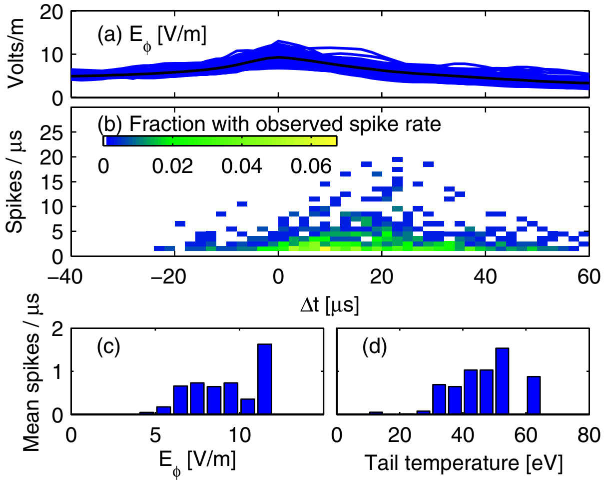

FIG. 4 (color online). (a) Reconnection electric fields for 80 discharges aligned to have peak E_ϕ at $\Delta t = 0$. (b) Histogram of observed spike events, the fraction out of all discharges which observed a given rate of spikes versus time relative to the peak E_ϕ. (c) Mean spike rate versus electric field, i.e., the total spikes observed given at particular electric field, divided by the total time elapsed with that electric field, divided by 4 probes. (d) Mean spike rate versus tail temperature.

tion time scale (microseconds). We find excellent correlation between the reconnection electric field and the effective temperature $[(d \log f / d\mathcal{E})^{-1}]$ of energetic electrons ($\mathcal{E} \sim 10T_e$), finding that it rises to the range of 50 eV during the reconnection events. We also estimate that these high energy electrons (with $\mathcal{E} \geq 100$ eV) comprise ~0.3% of the total density and carry ~5% of the plasma current during reconnection.

Figure 4 shows the statistical connection among holes, electric fields, and energetic particles, based on a study of approximately 80 discharges. To quantify the presence of the holes, we measure the hole rate, i.e., holes observed by a probe per microsecond. In Fig. 4(a), we have aligned the reconnection events for the discharges based on the maximum toroidal electric field. Figure 4(b) shows 2D histogram of the associated spike observations, indicating the fraction of discharges which observe the given rate of holes versus time; here the time axis is relative to the peak of the reconnection event. The spikes are clearly associated with the reconnection events, but note the delay between peak electric fields and peak hole observations. In Fig. 4(c), we show the mean hole rates given a specified toroidal electric field, and in Fig. 4(d), we show the mean spike rates given a specified tail temperature. These demonstrate a clear correlation among elevated electric fields, energetic electron creation, and hole observations.

Future work will continue to study the cause and effect among holes, fast electrons, and magnetic reconnection. Naively, these holes will not likely contribute substantial *direct* anomalous resistivity to the plasma, as their high velocity will limit interaction with ion populations. Instead, since the holes likely evolve from strong electron-electron instabilities, they will primarily work to transfer momentum from fast to slow electrons. This may, however, indirectly modify plasma resistivity, as the collisional resistivity depends strongly on the presence of the low-collisionality tail on the electron distribution function. This will be a subject of future investigations.

In conclusion, we report the identification of electron holes created during magnetic reconnection. Detailed study of individual holes has found that their typical sizes are a few ρ_e. The perpendicular size is in agreement with space observations and supports the idea that holes must always be at least a few ρ_e wide in order to retain magnetized electron dynamics. The holes are strongly associated with electron energization, evidenced by both their thermal velocity and their statistical connection to reconnection events and subsequent energetic particle production.

We thank Dr. M. Goldman for valuable discussions regarding the connection between fast electrons and parallel hole extent. This work was funded in part by DOE Junior Faculty Grant No. DE-FG02-06ER54878, CMPD Grant No. DEFC02-04ER54786, and an Oak Ridge Fusion Energy Sciences grant.

[1] I. Bernstein, J. Greene, and M. Kruskal, Phys. Rev. **108**, 546 (1957).
[2] H. Schamel, Phys. Rep. **140**, 161 (1986).
[3] J. R. Danielson *et al.*, Phys. Rev. Lett. **92**, 245003 (2004).
[4] H. Matsumoto *et al.*, Geophys. Res. Lett. **21**, 2915 (1994).
[5] R. E. Ergun *et al.*, Phys. Rev. Lett. **81**, 826 (1998).
[6] D. S. Montgomery *et al.*, Phys. Plasmas **9**, 2311 (2002).
[7] K. V. Roberts and H. L. Berk, Phys. Rev. Lett. **19**, 297 (1967).
[8] M. Oppenheim *et al.*, Phys. Rev. Lett. **83**, 2344 (1999).
[9] C. S. Ng *et al.*, Phys. Plasmas **13**, 055903 (2006).
[10] M. Goldman *et al.*, Phys. Rev. Lett. **99**, 145002 (2007).
[11] K. Saeki *et al.*, Phys. Rev. Lett. **42**, 501 (1979).
[12] H. Ji *et al.*, Phys. Rev. Lett. **92**, 115001 (2004).
[13] J. Drake *et al.*, Science **299**, 873 (2003).
[14] H. Matsumoto *et al.*, Geophys. Res. Lett. **30**, 1326 (2003).
[15] C. Cattell *et al.*, J. Geophys. Res. **110**, A01211 (2005).
[16] J. Egedal *et al.*, Phys. Rev. Lett. **98**, 015003 (2007).
[17] A. Kesich *et al.*, Rev. Sci. Instrum. **79**, 063505 (2008).
[18] A. M. Pointu, Appl. Phys. Lett. **50**, 316 (1987).
[19] M. Porkolab and M. V. Goldman, Phys. Fluids **19**, 872 (1976).
[20] H. Ikezi *et al.*, Phys. Fluids **14**, 1997 (1971).
[21] J. R. Franz *et al.*, Geophys. Res. Lett. **27**, 169 (2000).